Complementary filter design on the Special Euclidean group $SE(3)$

Grant Baldwin, Robert Mahony, Jochen Trumpf, Tarek Hamel & Thibault Cheviron

Abstract— This paper considers the problem of obtaining high quality pose estimation (position and orientation) from a combination of low cost sensors, such as an inertial measurement unit and vision sensor. A non-linear complementary filter is proposed that evolves on the Special Euclidean Group $SE(3)$. Exponential stability of the filter is proved. Simulation results are presented to illustrate simplicity and demonstrate the performance of the proposed approach. Experimental results reinforce the convergence of the filter.

Index Terms— Non-linear Filter, Complementary Filter, Special Euclidean Group.

I. INTRODUCTION

A fundamental problem in autonomous flight control of unmanned aerial vehicles is that of obtaining an accurate estimate of the position and orientation, or pose, of the vehicle. The underlying pose estimation problem is common to a wide range of applications including virtual reality, submersible robots and ground vehicles. Existing algorithms often rely on data obtained from military grade Inertial Measurement Units (IMU) and high quality camera systems with associated cost and export restrictions that prohibits commercial applications. By comparison, cheaper commercial grade IMUs commonly experience high levels of non-Gaussian noise in their gyrometer and accelerometer measurements that often leads to instability of classical Kalman and extended Kalman filter algorithms.

In prior work it has been shown that angular velocity and orientation (or attitude) can be estimated from the output of a low cost IMU [13], [8], [6] for a vehicle that is in quasi-stationary, or hover, flight. Conversely, translational position and velocity can not be estimated from a low cost IMU for more than a few seconds due to unbounded growth of errors [2]. Global Positioning System (GPS) can be used to bound error growth. However, such a strategy cannot be employed

G. Baldwin is with Departement of Engineering, Australian National University, ACT, 0200, Australia and National ICT Australia Ltd., `Grant.Baldwin@anu.edu.au`

R. Mahony is with Departement of Engineering, Australian National University, ACT, 0200, Australia, `Robert.Mahony@anu.edu.au`

J. Trumpf is with Department of Information Engineering, Research School of Information Science and Engineering, Australian National University, ACT, 0200, Australia and National ICT Australia Ltd., `Jochen.Trumpf@anu.edu.au`

T. Hamel is with I3S-CNRS Nice-Sophia Antipolis, France, `thamel@i3s.unice.fr`

T. Cheviron is with LRBA, DGA, Vernon and IRCCyN, UMR 6597, Ecole Centrale de Nantes/CNRS, Nantes, France, `Thibault.Cheviron@dga.defense.gouv.fr`

in situations where the GPS signal is unreliable, eg. indoors, urban canyon environments or in military environments, and there is considerable interest in algorithms that do not require GPS. Inertial vision systems are systems that combine IMU and on-board camera measurements for pose estimation [11], [7]. Two recent international conferences have had workshops on inertial vision systems [18], [4]. Classical approaches, such as linear and extended Kalman filter techniques [9], [12] have proven difficult to apply robustly with low quality sensor systems [13]. Nevertheless, most of the recent examples of autonomous aerial robotic vehicles over the last few years have relied heavily on the combination of inertial sensor and vision systems [5], [1], [15] and there is significant interest in developing simple robust estimators that use inertial and visual sensor systems for pose estimation.

In this paper we study the design of complementary filers on the special Euclidean group SE(3) to provide estimates of the pose and velocity of a rigid body. The work is an extension of the passive complementary filter developed on the orthogonal group SO(3) [8], [6]. The work draws from earlier work on attitude estimation that exploited the quaternion formulation [14], [17], [16]. We propose two filters; a direct complementary filter, and a non-linear passive complementary filter. The passive filter has a number of advantages over the direct filter in its stability and noise sensitivity. Simulations of the performance of the filters are provided.

Section II reviews the structure and properties of SE(3). Section III describes the proposed target system, including the analysis framework and sensor characteristics. A direct complementary filter is developed in section IV, followed by the development of a passive complementary filter in section V. Section VI discusses the practical concerns of implementing these filters via discrete integration. Section VII presents simulation results for the passive complementary filter, demonstrating its performance and characteristics. Section VIII presents experimental results confirming the behaviour of the filter on real world data.

II. BACKGROUND THEORY

Let $\{A\}$ denote an inertial frame attached to the earth, such that e_3 points vertically down. We consider the problem of estimating the pose of a body-fixed-frame, $\{B\}$, that is attached to a vehicle of interest. The vehicle is equipped with an inertial measurement unit (IMU) and camera. We assume for simplicity that IMU and camera are co-located at the origin of the body-fixed-frame, denoted $p \in \{A\}$, expressed as a point in the inertial frame. The attitude of the vehicle is

given by a rotation matrix R that represents the attitude of $\{B\}$ with respect to $\{A\}$. Positions and vectors expressed in the inertial frame, $\{A\}$, will be denoted by lower case letters while positions and vectors expressed in other frames will be denoted by upper case letters. Let $v \in \{A\}$ denote the linear velocity and $\Omega \in \{B\}$ denote the angular velocity of the body-fixed-frame. Note that it is common to work with the linear velocity in the inertial frame and the angular velocity in the body-fixed-frame.

The standard expression for the kinematics of $\{B\}$ is

$$\dot{p} = v, \tag{1a}$$
$$\dot{R} = R\Omega_\times \tag{1b}$$

where $\Omega_\times$ is the skew symmetric matrix

$$\Omega_\times = \begin{pmatrix} 0 & -\Omega_3 & \Omega_2 \\ \Omega_3 & 0 & -\Omega_1 \\ -\Omega_2 & \Omega_1 & 0 \end{pmatrix} \tag{2}$$

In this paper we will also need to work with the full body fixed-frame-representation of the body-fixed-frame kinematics. Let

$$P = -R^T p, \qquad V = R^T v, \qquad \omega_\times = (R^T\Omega)_\times$$

denote the position and translational velocity of the vehicle in the body fixed frame. Note that the position is the origin of $\{A\}$ expressed in $\{B\}$. Equation 1a becomes

$$\dot{P} = \Omega_\times P - V. \tag{3}$$

The pose of the body-fixed-frame, (R, p), comprises both the attitude and position of $\{B\}$ relative to an inertial frame. The pose can interpreted as an element of the Special Euclidean group of dimension three, SE(3). We represent an element of SE(3) by a matrix

$$T = \begin{pmatrix} R & p \\ 0 & 1 \end{pmatrix} \in \mathbb{R}^{4 \times 4} \tag{4}$$

This format, commonly known as homogenous coordinates, preserves the group structure of SE(3) with the GL(4) operation of matrix multiplication. The inverse element associated with T is

$$T^{-1} = \begin{pmatrix} R^T & -R^T p \\ 0 & 1 \end{pmatrix} = \begin{pmatrix} R^T & P \\ 0 & 1 \end{pmatrix} \tag{5}$$

The kinematics of $T \in$ SE(3) in matrix form are

$$\dot{T} = T\mathbf{A} \tag{6}$$

where $\mathbf{A}$ denotes the body-fixed-frame velocity of the system

$$\mathbf{A} = \begin{pmatrix} \Omega_\times & V \\ 0 & 0 \end{pmatrix} \in \mathfrak{se}(3) \tag{7}$$

It is easily verified that Eq. 7 is a matrix representation of the kinematics Eqn's. 1.

We think of $\mathbf{A}$ as an element of the Lie-algebra of SE(3) denoted $\mathbf{A} \in \mathfrak{se}(3)$, where $\mathfrak{se}(3)$ is identified with the subset of 4×4 matrices with an upper left skew symmetric 3×3 block and bottom row zero. The correspondence of body-fixed-frame velocities (Ω, V) to an element $\mathbf{A} \in \mathfrak{se}(3)$ is denoted by a wedge operator

$$\mathbf{A} = (\Omega, V)^\wedge \tag{8}$$

Note that the wedge operator associates an element of $\mathfrak{se}(3)$ with a particular frame of reference. Thus, $\mathbf{A}$ in Eq. 8 is associated with the body-fixed-frame $\{B\}$ since Ω and V are expressed in $\{B\}$. The adjoint operator, $\mathrm{Ad}_T : \mathfrak{se}(3) \to \mathfrak{se}(3)$ is defined as

$$\mathrm{Ad}_T\, \mathbf{A} := T\mathbf{A}T^{-1}. \tag{9}$$

The adjoint operator acts to change the frame of reference associated with an element of the Lie-algebra. Thus,

$$\mathrm{Ad}_T\, (\Omega, V)^\wedge = (\omega, v)^\wedge.$$

We define an inner product and induced matrix norm on the set of $\mathbb{R}^{n \times n}$ matrices

$$\begin{aligned} \langle A, B \rangle &:= \tfrac{1}{2}\,\mathrm{tr}(A^T B) \\ \langle A, A \rangle &= \tfrac{1}{2}\,\mathrm{tr}(A^T A) = \|A\|_F^2 \end{aligned} \tag{10}$$

where $\|(\cdot)\|_F$ is the classical Frobenius norm.

Let $\mathbb{P}_a$ and $\mathbb{P}_s$ be projection operators decomposing an matrix $M \in \mathbb{R}^{n \times n}$ into an anti-symmetric component $\mathbb{P}_a(M)$ and a symmetric components $\mathbb{P}_s(M)$, given by

$$\mathbb{P}_a(M) = \frac{1}{2}(M - M), \quad \mathbb{P}_s(M) = \frac{1}{2}(M + M)$$

III. FILTER DESIGN AND ERROR CRITERIA FOR ESTIMATION ON SE(3)

In this section, a detailed analysis of the natural error coordinates and cost functions are presented for an estimation problem on SE(3).

Let $\{E\}$ denote a new frame of reference representing the best estimate of $\{B\}$. We represent the frame $\{E\}$ by an element

$$\hat{T} := \begin{pmatrix} \hat{R} & \hat{p} \\ 0 & 1 \end{pmatrix} \in \text{SE}(3)$$

The kinematics of $\hat{T}$ are given by

$$\dot{\hat{T}} = \hat{T}\hat{\mathbf{A}} = \hat{T}\left(\hat{\Omega}, \hat{V}\right)^\wedge \tag{11}$$

$$\tag{12}$$

where $\hat{V} \in \{E\}$ and $\hat{\Omega} \in \{E\}$ denote the linear and angular velocities of frame $\{E\}$. The goal of the estimator design is to choose suitable values for $(\hat{\Omega}, \hat{V})$, as functions of the measured variables, to ensures that $\hat{T}(t) \to T(t)$.

A. System Measurements

The sensor suite considered consists of an inertial measurement unit (IMU) along with a camera. The IMU provides direct measurement of angular velocity of the body-fixed-frame $\{B\}$. We assume that the camera is observing a known target and use a classical pose estimation algorithm to estimate the pose of $\{B\}$. Linear velocity, though not measured directly, can be reconstructed from the integral

of acceleration measurements and the derivative of position component of pose measurements,

Since the present paper is an initial investigation we will assume a simple measurement model that does not include bias terms and calibration errors that commonly occur for low-cost sensor systems. The measurement model used is

$$\Omega_y = \Omega + n_\Omega(t),$$
$$V_y = V + n_V(t),$$
$$R_y = R^T_{n_R(t)}R,$$
$$P_y = P + n_p(t),$$

where $n_{(\cdot)}(t)$ denotes a centred Gaussian noise process. The pose estimate algorithms used for the reconstruction of (R_y, P_y) are computationally demanding and these estimates are low bandwidth. The IMU data is high bandwidth while a high-bandwidth estimate of the linear velocity must also be estimated to ensure good properties of the resulting filter.

IV. DIRECT FILTER

The coordinates T of $\{B\}$ relative to $\{A\}$ may be interpreted as a coordinate transformation

$$T : \{B\} \to \{A\} : \qquad \begin{pmatrix} x \\ 1 \end{pmatrix} \mapsto T \begin{pmatrix} x \\ 1 \end{pmatrix} = \begin{pmatrix} Rx + p \\ 1 \end{pmatrix}$$

The estimator frame coordinate frame transformation $\hat{T} : \{E\} \to \{A\}$ and its inverse $\hat{T}^{-1} : \{A\} \to \{E\}$ are defined analogously. Thus we can construct an error coordinate transformations

$$\bar{T} = T^{-1}\hat{T} : \{E\} \to \{B\}$$

In attitude and position one has

$$\bar{T} = \begin{pmatrix} \bar{R} & \bar{p} \\ 0 & 1 \end{pmatrix}$$
$$\bar{R} = R^T\hat{R}, \qquad \bar{p} = R^T(\hat{p} - p)$$

If $\bar{T} \to I$, where I denotes the identity matrix, then $\hat{T} \to T$. The cost function considered in the sequel is

$$\mathcal{L}(\bar{T}) := ||I - \bar{T}||^2_F. \tag{13}$$

Set $\bar{P} = -\bar{R}^T\bar{p} = \hat{R}^T(p - \hat{p})$. Noting that $\frac{d}{dt}(\hat{T}\hat{T}^{-1}) = 0$, yields the following kinematics

$$\dot{\bar{T}} = \bar{T}\hat{\mathbf{A}} - \mathbf{A}\bar{T} \tag{14}$$
$$= \bar{T}(\hat{\mathbf{A}} - \mathrm{Ad}_{\bar{T}^{-1}}\mathbf{A})$$
$$= \bar{T}\bar{\mathbf{A}}$$

where $\bar{\mathbf{A}} = (\bar{\Omega}, \bar{V})^\wedge \in \mathfrak{se}(3)$ and

$$\bar{\Omega}_\times = \hat{\Omega}_\times - \mathrm{Ad}_{\bar{R}^T}\Omega_\times \tag{15}$$
$$\bar{V} = \hat{V} - \bar{R}^TV + \mathrm{Ad}_{\bar{R}^T}(\Omega)\bar{P} \tag{16}$$

Theorem 1 (Direct Filter on SE(3)*):* Consider the system defined in Section III with error measure $\bar{T}$, given by Eq. 14, along with $\hat{\Omega}$ and $\hat{V}$ given by:

$$\hat{\Omega} = \mathrm{Ad}_{\bar{R}_y}(\Omega_y) + K_R\mathbb{P}_a(\bar{R})^T \tag{17}$$
$$\hat{V} = \bar{R}^T_yV_y + K_P\bar{P} \tag{18}$$

where $(R_y, P_y, \Omega_y, V_y)$ are noise free measurements of the true system in the body fixed frame, with $\bar{R}_y = R^T_y\hat{R}$. Then, for any initial condition such that

$$\mathrm{tr}(\bar{R}(0)) \neq -1$$

$||I - \bar{T}||_F$ converges exponentially to zero. It follows that $\bar{T} \to I$ exponentially and $\hat{R} \to R$ and $\hat{p} \to p$.

Proof: [Theorem 1] Recall the dynamics of the deviation $\bar{T}$

$$\dot{\bar{T}} = \bar{T}\mathbf{A} - \hat{\mathbf{A}}\bar{T}$$

Define the following candidate Lyapunov function $\mathcal{L}$

$$\mathcal{L} = \tfrac{1}{2}||I - \bar{T}||^2_F$$
$$= \mathrm{tr}(I - \bar{R}) + \tfrac{1}{2}||\bar{p}||^2_2$$
$$= \mathcal{L}_R + \mathcal{L}_P,$$

where $\mathcal{L}_R = \mathrm{tr}(I - \bar{R})$ and $\mathcal{L}_P = \tfrac{1}{2}||\bar{p}||^2_2 = \tfrac{1}{2}||\bar{P}||^2_2$.

Taking the time derivative of $\mathcal{L}_R$, substituting for $\hat{\Omega}$ from Eq. 17 and setting $R_y \equiv R$ and $\Omega_y \equiv \Omega$ yields

$$\dot{\mathcal{L}}_R = -\mathrm{tr}(\dot{\bar{R}})$$
$$= -\mathrm{tr}(\bar{R}(\hat{\Omega}_\times - \mathrm{Ad}_{\bar{R}^T}\Omega_\times))$$
$$= -\mathrm{tr}(\bar{R}(\mathrm{Ad}_{\bar{R}^T}\Omega_\times + K_R\mathbb{P}_a(\bar{R})^T - \mathrm{Ad}_{\bar{R}^T}\Omega_\times)))$$
$$= -K_R\mathrm{tr}(\bar{R}\mathbb{P}_a(\bar{R})^T)$$

Given that $\bar{R} = \mathbb{P}_s(\bar{R}) + \mathbb{P}_a(\bar{R})$, and that $\mathrm{tr}(\mathbb{P}_s(\bar{R})\mathbb{P}_a(\bar{R})^T) = 0$, the derivative of $\mathcal{L}_R$ becomes

$$\dot{\mathcal{L}}_R = -K_R||\mathbb{P}_a(\bar{R})||^2_F$$

Let, $(\bar{\theta}, \bar{a})$ denote the angle-axis coordinates of $\bar{R}$. One has [10]

$$\bar{R} = \exp(\bar{\theta}\bar{a}_\times), \qquad \log(\bar{R}) = \bar{\theta}\bar{a}_\times$$
$$\cos(\bar{\theta}) = \tfrac{1}{2}(\mathrm{tr}(\bar{R}) - 1), \qquad \bar{a}_\times = \tfrac{1}{\sin(\bar{\theta})}\mathbb{P}_a(\bar{R}) \tag{19}$$

The cost function $\mathcal{L}_R$ may be written

$$\mathcal{L}_R = \mathrm{tr}(I - \bar{R}) = 2(1 - \cos(\bar{\theta})) = 4\sin(\bar{\theta}/2)^2. \tag{20}$$

Substituting for $\sin(\bar{\theta})\bar{a}_\times = \mathbb{P}_a(\bar{R})$ gives

$$\dot{\mathcal{L}}_R = -K_R\sin^2(\bar{\theta})||\bar{a}_\times||^2_F = -K_R\sin^2(\bar{\theta})$$
$$= -4K_R\sin^2(\bar{\theta}/2)\cos^2(\bar{\theta}/2) = -K_R\cos^2(\bar{\theta}/2)\mathcal{L}_R.$$

For $\theta \neq \pm\pi$ then $\mathcal{L}_R$ is exponentially decreasing to zero. Note that $\theta = \pm\pi$ if and only if $\mathrm{tr}(\bar{R}) = -1$.

Taking the derivative of $\mathcal{L}_P$ and setting $V_y \equiv V$ and $P_y \equiv P$ yields:

$$\dot{\mathcal{L}}_P = \bar{P}^T\dot{\bar{P}}$$
$$= \bar{P}^T(-\hat{V} + \bar{R}^TV - \hat{\Omega}\bar{P})$$

Given that $\bar{P}^T\hat{\Omega}_\times\bar{P} = 0$ and substituting $\hat{V}$ from Eq. 18

$$\dot{\mathcal{L}}_P = -K_P||\bar{P}||^2_2 = -2K_P\mathcal{L}_P$$

This insures $\mathcal{L}_P$ converges exponentially to zero and therefore $\hat{T} \to T$ exponentially. The result follows directly. ∎

In this proof we have assumed ideal measurements $(R_y, P_y, \Omega_y, V_y)$. Clearly, in such a case it is unnecessary to filter, however, even in the presence of noisy measurements

the expected response of the proposed filter will be as given in the theorem.

The output of the direct complementary filter estimator suffers from coupling between measurement errors. Firstly, the angular velocity estimate, Eq. 17, is adjointed by the instantaneous rotational error, $\bar{R}$. The instantaneous rotation error is derived from the measurement R_y, which is typically corrupted by low frequency noise. This corrupts the high frequency angular velocity estimate with a low frequency noise. Secondly, the linear velocity estimate, Eq. 18, will propagate low frequency noise present in R_y by both the measurement term, $\bar{R}_y$, and the innovation term, $-K_P \bar{P} = -K_P \hat{R}^T(\hat{p} - p) = -K_P(\bar{R}^T P - \hat{P})$.

V. COMPLEMENTARY FILTER ON $\mathrm{SE}(3)$

The problems associated with the direct filter can be linked to the interpretation of the error term $\bar{T} = T^{-1}\hat{T}$. The error term was interpreted as a coordinate transformation $\bar{T} : \{E\} \to \{B\}$. However, the error can be viewed as the coordinates of $\{E\}$ expressed with respect to the body-fixed-frame $\{B\}$. That is, $\bar{T}$ is associated with the frame of reference $\{B\}$. The non-linear geometry of the Lie-group $\mathrm{SE}(3)$ introduces a complexity that is not present in classical linear filtering; the error $\bar{T}$ is defined with respect to the moving frame $\{B\}$ and not the inertial frame $\{A\}$. This causes undesirable coupling of system dynamics into the error term. In particular, when the system undergoes rotation there is a corresponding variation of the translational error that is due to the change of reference frame and not a translational error. The solution is to represent the error term $\bar{T}$ in the inertial frame.

Analogous to the adjoint operator Ad_T that changes frames of reference associated with elements in $\mathfrak{se}(3)$, there is an inner-automorphism operator

$$\mathcal{I}_T : \mathrm{SE}(3) \to \mathrm{SE}(3) \; \mathcal{I}_T(Q) := TQT^{-1}, \qquad T \in \mathrm{SE}(3),$$

that acts to change the frame of reference associated with an element of the Lie-group $\mathrm{SE}(3)$. In particular, if $\bar{T}$ is associated with $\{B\}$, and $T \in \mathrm{SE}(3)$ is the coordinates of $\{B\}$ with respect to an inertial frame $\{A\}$, then $\mathcal{I}_T(\bar{T})$ is associated with the inertial frame $\{A\}$.

Let

$$\tilde{T} := \mathcal{I}_T(\bar{T}) = \hat{T}T^{-1} \tag{21}$$

denote the error $\bar{T}$ represented in the inertial frame of reference. In the coordinate representation of $\tilde{T}$ one has

$$\tilde{T} = \begin{pmatrix} \tilde{R} & \tilde{p} \\ 0 & 1 \end{pmatrix}$$

where

$$\tilde{R} = \hat{R}R^T$$
$$\tilde{p} = \hat{p} - \tilde{R}p$$

It is straightforward to verify that

$$\tilde{P} = -\tilde{R}^T \tilde{p} = R(\hat{P} - P).$$

Note that $\tilde{T}$ does not have an interpretation as a mapping operator.

The goal of the filter is to drive the error term $\tilde{T} \to I$. Analogous to the previous case, we consider the cost function Eq. 13,

$$\mathcal{L}(\tilde{T}) := \frac{1}{2}\|I - \tilde{T}\|_F^2.$$

The kinematics of $\tilde{T}$ are

$$\dot{\tilde{T}} = \tilde{T}\,\mathrm{Ad}_T(\hat{\mathbf{A}} - \mathbf{A}),$$
$$= \tilde{T}\tilde{\mathbf{A}}, \tag{22}$$

where $\tilde{\mathbf{A}} = \left(\tilde{\Omega}, V\right)^\wedge \in \mathfrak{se}(3)$ and

$$\tilde{\Omega}_\times = \mathrm{Ad}_R(\hat{\Omega} - \Omega)_\times$$
$$\tilde{V} = R(\hat{V} - V) + \tilde{\Omega}_\times p$$

Theorem 2 (Complementary filter on $\mathrm{SE}(3)$*):* Consider the system defined in section III with deviation measure $\tilde{T}$, given by Eq. 21, along with $\hat{\Omega}$ and $\hat{V}$ given by

$$\hat{\Omega}_\times = \Omega_{y\times} - K_R\,\mathrm{Ad}_{R^T}\,\mathbb{P}_a(\tilde{R}_y) \tag{23}$$
$$\hat{V} = V_y - (\hat{\Omega} - \Omega_y)_\times \hat{P} + K_P(\hat{P} - P_y) \tag{24}$$

where $(R_y, \; P_y, \; \Omega_y, \; V_y)$ are noise free measurements of the true system in the body fixed frame, with $\tilde{R}_y = \hat{R}R_y^T$. Then, for any initial condition such that

$$\mathrm{tr}(\tilde{R}(0)) \neq -1$$

$\|I - \tilde{T}\|_F^2$ converges exponentially to zero. It follows that $\tilde{T} \to I$ exponentially and $\hat{R} \to R$ and $\hat{p} \to p$.

Proof: [Theorem 2] Recall the dynamics of the deviation $\tilde{T}$ from Eq. 22. Define the following candidate Lyapunov function $\mathcal{L}$

$$\begin{aligned}\mathcal{L} &= \tfrac{1}{2}\|I - \tilde{T}\|_F^2 \\ &= \mathrm{tr}(I - \tilde{R}) + \tfrac{1}{2}\|\tilde{p}\|_2^2 \\ &= \mathcal{L}_R + \mathcal{L}_P\end{aligned} \tag{25}$$

Where again $\mathcal{L}_R = \mathrm{tr}(I - \tilde{R})$ and $\mathcal{L}_P = \frac{1}{2}\|\tilde{p}\|_2^2 = \frac{1}{2}\|\tilde{P}\|_2^2$.

Taking the time derivative of $\mathcal{L}_R$, substituting for $\hat{\Omega}$ from Eq. 23 and letting $R_y \equiv R$ and $\Omega_y \equiv \Omega$ yields $\dot{\mathcal{L}}_R = -K_R\|\mathbb{P}_a(\tilde{R})\|_F^2$, and by analogous argument to that used in the previous proof, $\mathcal{L}_R$ is exponentially decreasing to zero.

Taking the time derivative of $\mathcal{L}_P$, letting $V_y \equiv V$ and $P_y \equiv P$ yields

$$\begin{aligned}\dot{\mathcal{L}}_P &= \tilde{P}^T\dot{\tilde{P}} \\ &= \tilde{P}^T(-R\hat{V} + RV - R(\hat{\Omega} - \Omega)_\times \hat{P})\end{aligned}$$

substituting for $\hat{V}$ from Eq. 24

$$\dot{\mathcal{L}}_P = -K_P\|\tilde{P}\|_2^2 = -2K_P\mathcal{L}_P$$

This insures $\mathcal{L}_P$ converges exponentially to zero and therefore $\hat{T}$ converges exponentially to T. ∎

The complementary filter avoids the problems identified with the direct filter. The estimation dynamics Eq. 23 and Eq. 24 contain no cross terms between measurements.

Changes between frames are avoided by making error comparisons in the inertial frame.

A disadvantage of the complementary filter formulation is the increased complexity in the linear velocity estimate, Eq. 24, with the term $(\hat{\Omega} - \Omega_y)_\times \hat{P}$. This cross product between the position of origin in the body fixed frame and the error in angular velocity couples the linear velocity to orientation, as a correction for the convergence in orientation. However, as will be demonstrated in the next section, this term can be omitted without affecting the exponential convergence of the filter.

VI. PRACTICAL IMPLEMENTATION

The filters developed in the prior two sections may be implemented using any sensible interpolation scheme. In this section we discuss implementing such integration with complementary filter described in section V.

First we address error coupling in the translation term from the angular velocity measurement. Recall Eq. 24:

$$\hat{V} = V_y - (\hat{\Omega} - \Omega_y)_\times \hat{P} + K_P(\hat{P} - P_y)$$

The $(\hat{\Omega} - \Omega_y)_\times \hat{P}$ term will not exactly cancel with the $(\hat{\Omega} - \Omega)_\times \hat{P}$ term in the Lyapunov function due to the noise in the measurement Ω_y. While zero mean random noise will ensure that the expected value of the resulting filter has the desired properties, the cross term increases the high frequency noise in the position estimate. We may eliminate this noise in the position estimate by discarding the problematic terms, by using a modified form of the estimation equations.

Proposition 3 (Convergence for altered $\hat{V}$): Consider the statement of Theorem 2. Let α and β be two positive constants such that

$$\mathcal{L}_R < \frac{1}{2}\alpha^2 e^{-2\beta t}$$

over a bounded translation area such that

$$||P(t)|| \leq ||P_{max}||, \qquad \text{for all } t.$$

The estimation dynamics of Eq. 23 and

$$\hat{V} = V_y + K_P(\hat{P} - P_y) \qquad (26)$$

instead of Eq. 24 then the exponential convergence of $\tilde{T}$ remains valid.

Proof: [Proposition 3] Recall the deviation measure from Eq. 21. Let $\mathcal{L} = \frac{1}{2}||\tilde{P}||^2$ be a candidate Lyapunov function

$$
\begin{aligned}
\dot{\mathcal{L}} =&\ \tilde{P}^T(-R\hat{V} + RV - R(\hat{\Omega} - \Omega)_\times \hat{P}) \\
\dot{\mathcal{L}} =&\ \tilde{P}^T(-K_P\tilde{P}_y - R(\hat{\Omega} - \Omega)_\times P) \\
\dot{\mathcal{L}} =&\ -K_P||\tilde{P}||^2 - \tilde{P}^T R(\hat{\Omega} - \Omega)_\times P \\
\dot{\mathcal{L}} \leq&\ -2K_P\mathcal{L} - \sqrt{2\mathcal{L}}\,||(\Omega - \hat{\Omega})_\times||\,||P_{max}||
\end{aligned}
$$

Given that $||(\hat{\Omega} - \Omega)_\times||$ is bounded by $K_R \alpha e^{-\beta t}$, $\dot{\mathcal{L}}$ can be bounded as follows

$$
\begin{aligned}
\dot{\mathcal{L}} \geq&\ -2K_P\mathcal{L} - \sqrt{2\mathcal{L}}K_R \alpha e^{-\beta t}||P_{max}|| \\
\dot{\mathcal{L}} \leq&\ -2K_P\mathcal{L} + \sqrt{2\mathcal{L}}K_R \alpha e^{-\beta t}||P_{max}||
\end{aligned}
$$

Let $W = \sqrt{2\mathcal{L}}$, with $\dot{W} = \frac{\dot{\mathcal{L}}}{2W}$. Substituting, we have

$$
\begin{aligned}
\dot{W} \geq&\ -K_P\frac{W}{2} - \frac{1}{2}K_R \alpha e^{-\beta t}||P_{max}|| \\
\dot{W} \leq&\ -K_P\frac{W}{2} + \frac{1}{2}K_R \alpha e^{-\beta t}||P_{max}||
\end{aligned}
$$

Let

$$
\begin{aligned}
\dot{W}_1 =&\ -K_P\frac{W}{2} - \frac{1}{2}K_R \alpha e^{-\beta t}||P_{max}|| \\
\dot{W}_2 =&\ -K_P\frac{W}{2} + \frac{1}{2}K_R \alpha e^{-\beta t}||P_{max}||
\end{aligned}
$$

Then $W_1 < W < W_2$ and, Clearly, if both W_1 and W_2 converge to zero, then W converges to zero. It is straight forward to show that

$$
\begin{aligned}
W_1 =&\ e^{-K_P t}W_1(0) \\
&\ - \frac{K_R \alpha ||P_{max}||}{2}(e^{-\beta t} - e^{-K_P t})
\end{aligned}
$$

As β and K_P are both greater than zero, the exponential terms converge to zero. Analogously, W_2 converges to zero and thus W converges to zero. Since W_1 and W_2 both converge exponentially to zero, W converges exponentially to zero. ∎

As will become apparent from the figures in section VII, this modified form of $\hat{V}$ allows a temporary divergence in the position estimate while the system undergoes a transition to correct large orientation error. The selection of gains K_P and K_R, addressed in section VI-B, allows this deviation to be controlled to an extent.

A. Discrete integration on SE(3)

Euler integration is the simplest form of numerical integration. The value over time is incremented as if the derivative is constant at the last received value between samples.

$$y_{t+\tau} = y_t + \tau \dot{y}(t)$$

Where τ is the time step. In SE(3), the Euler step must be constrained to lie on the Lie group. A simple choice is

$$T(t + \tau) = \exp(\tau \mathbf{A}(t))T(t)$$

where exp is the matrix exponential. Note that there are explicit forms for the matrix exponential on SE(3) based on Rodriguez formulae that are computationally tractable. For our filters one obtains

$$
\begin{aligned}
\hat{\mathbf{A}}(t) =&\ \left(\hat{\Omega}(t), \hat{V}(t)\right)^\wedge \\
\hat{T}(t + \tau) =&\ \exp(\tau \hat{T}(t)\hat{\mathbf{A}}(t)\hat{T}(t)^{-1})\hat{T}(t)
\end{aligned}
$$

where we multiply by the exponential of $\text{Ad}_{T(t)}\,\hat{\mathbf{A}}(T)$ corresponding to $\dot{\hat{T}}^{-1} = \hat{T}^{-1}\text{Ad}_{\hat{T}}\,\hat{A}$.

As an alternative to Euler integration, we may use Runge-Kutta integration to attempt to eliminate this high frequency noise. The second-order method [19], which integrates by an estimate of the derivative at the midpoint of the step, is

$$
\begin{aligned}
y_{t+\tau} =&\ y_t + k_2 \\
k_2 =&\ \tau\,\mathrm{f}(t + \frac{1}{2}\tau, y_t + \frac{1}{2}k_1) \\
k_1 =&\ \tau\,\mathrm{f}(t, y_t)
\end{aligned}
$$

where τ is again the time step. For our system in SE(3) we make the simplification that $\mathrm{f}(t, y(t))$ is independent of t, as

the estimator converges to the true state without additional kinematics.

$$T(t + \tau) = \exp(\tau \tfrac{d}{dt}(\exp(\tfrac{1}{2}\tau \mathbf{A}(t))T(t))T(t)$$

For implementation in our system, this translates into

$$
\begin{aligned}
\hat{\Omega}(t)_\times =\ & \Omega_y(t)_\times + K_R \, \mathrm{Ad}_{R(t)^T} \, \mathbb{P}_a(\tilde{R}_y(t))^T \\
\hat{V}(t) =\ & V_y(t) - (\hat{\Omega}(t) - \Omega_y(t))_\times \hat{P}(t) \\
& - K_P(\hat{P}(t) - P(t)) \\
\hat{\mathbf{A}}(t) =\ & (\hat{\Omega}(t), \hat{V}(t))^\wedge \\
\hat{T}(t + \tfrac{1}{2}\tau) =\ & \exp(\tfrac{1}{2}\hat{T}(t)\hat{\mathbf{A}}(t)\hat{T}(t)^{-1})T(t) \\
\hat{\Omega}(t + \tfrac{1}{2}\tau) =\ & \Omega_y(t)_\times + K_R \, \mathrm{Ad}_{R(t+\frac{1}{2}\tau)^T} \, \mathbb{P}_a(\tilde{R}_y(t))^T \\
\hat{V}(t + \tfrac{1}{2}\tau) =\ & V_y(t) - (\hat{\Omega}(t + \tfrac{1}{2}\tau) - \Omega_y(t))_\times \hat{P}(t + \tfrac{1}{2}\tau) \\
& + K_P(\hat{P}(t + \tfrac{1}{2}\tau) - P_y(t)) \\
\hat{\mathbf{A}}(t + \tfrac{1}{2}\tau) =\ & \left(\hat{\Omega}(t + \tfrac{1}{2}\tau), \hat{V}(t + \tfrac{1}{2}\tau)\right)^\wedge \\
\hat{T}(t + \tau) =\ & \exp(\tau \hat{T}(t + \tfrac{1}{2}\tau)\hat{\mathbf{A}}(t + \tfrac{1}{2}\tau)\hat{T}(t + \tfrac{1}{2}\tau)^{-1})\hat{T}(t)
\end{aligned}
$$

where again we make the adjustment of the direction of integration as previous. While this method reduces the high frequency noise from Euler integration, it still incorporates the same noise in the position estimate.

B. Gain selection

The values of the gains K_P and K_R correspond to the cross over frequencies between the response to the pose measurements R_y and P_y and the velocity measurements Ω_y and V_y. Values of the gains corresponds to the crossover frequencies in radians per second. Values will typically be selected based on analysis of the sensors used, but will lie somewhere between zero and the Nyquist frequency of the sampling rate of the pose measurement. Values higher than the Nyquist frequency of the pose measurement may be used to aggressively counteract off-set errors occurring due to dropped frames or missing pose measurements when tracking moving targets.

When employing the modified form of $\hat{V}$, the system will undergo a divergence in the position estimate during periods of high angular velocity. The ratio K_P/K_R determines the relative timing of this divergence appearing in the position estimate. A high value will delay the divergence and spread it over time. Conversely a low value may cause an immediate, sharp, spike.

VII. SIMULATION RESULTS

The proposed design of the complementary filter has been simulated using MATLAB 7.1. Both the system and estimator are initialised to random elements of a translational subspace of $SE(3)$

- The rotation, R, is initiated to a rotation of $\pi - 0.1$ around random axis selected uniformly.
- The position, p, is a selected from the cube $(-10..10, -10..10, -10..10)$ under a uniform random distribution.

Repeated testing using this selection identifies numerical errors that may not be apparent when either the target or estimate is initialised to the identity matrix or other elements of $SE(3)$ inside the unit cube.
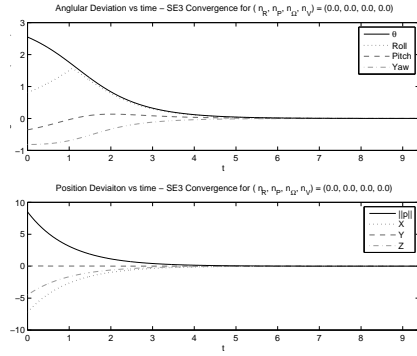

Fig. 1. $\tilde{T}$ vs. time (in iterations) for $SE(3)$ convergence from random element to another random element with no sensor noise. Typical result from repeated testing.
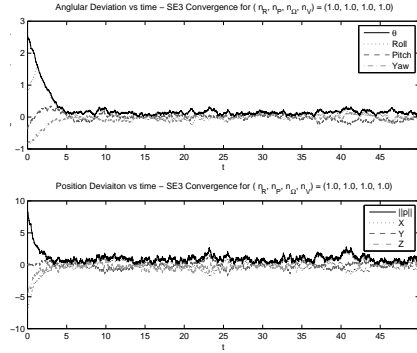

Fig. 2. $\tilde{T}$ vs. time (in iterations) for $SE(3)$ convergence from random element to another random element with noise variances of 1.0 on all sensors. Typical result from repeated testing.

Simulations were performed using a variety of white noise processes and both the original and modified (proposition 3) complementary filter dynamics. All images depict simulations of the same randomly generated system with changes only to the filter parameters. The filter parameters are $K_R = 1$, $K_P = 1$, $\tau = 10^{-1}$, with no sensor noise or bias and iteration via Euler integration unless otherwise specified. Noise variances have been selected to be excessively high to create adverse conditions. Noise was added to measurements as follows

- R_y: Noise as a rotation by θ radians around a uniform randomly selected axis, where θ is drawn from a zero mean Gaussian process with a specified variance in radians.
- P_y, Ω_y and V_y: Noise added as a three independent component vector drawn from a Gaussian process with a specified variance in units.

All noise variance are specified independently. Typical results for tests with no noise are indicate in figure 1.

The system proved highly stable under noise on the measurements R_y, P_y, and V_y, yet sensitive to noise in Ω_y. Despite this, when noise is applied to all sensors, the filter achieves a good degree of convergence as depicted in figure 2. Contrasting the results of figures 3 and 4, it is clear that the majority of the disturbance is due to the noise on the angular velocity sensor. When this is removed, the filter is
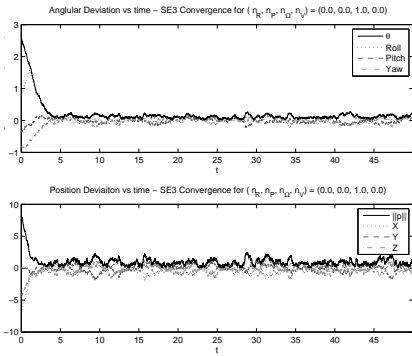
Fig. 3. $\tilde{T}$ vs. time (in iterations) for SE(3) convergence from random element to another random element with noise variances of 1.0 on only the angular velocity sensor. Typical result from repeated testing.
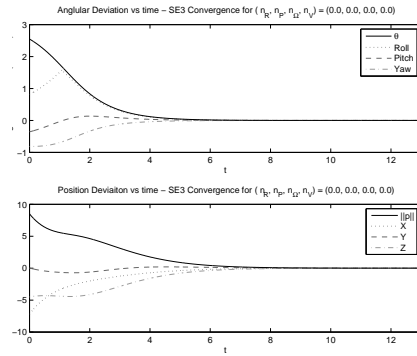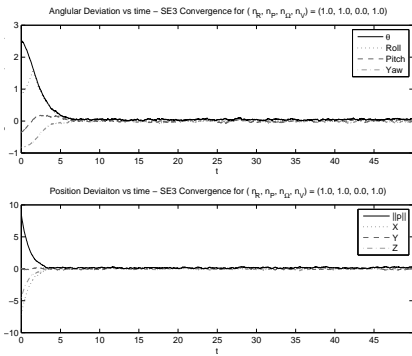

Fig. 4. $\tilde{T}$ vs. time (in iterations) for SE(3) convergence from random element to another random element with noise variances of 1.0 on all sensors except the angular velocity sensor. Typical result from repeated testing.

Fig. 5. $\tilde{T}$ vs. time (in iterations) for SE(3) convergence from random element to another random element with no sensor noise using $\hat{V}$ of proposition 3. Typical result from repeated testing.
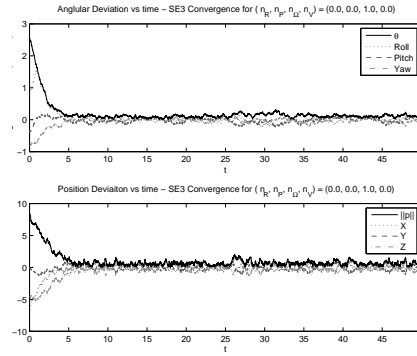

Fig. 6. $\tilde{T}$ vs. time (in iterations) for SE(3) convergence from random element to another random element with noise variances of 1.0 on only the angular velocity sensor using $\hat{V}$ of proposition 3. Typical result from repeated testing.

comparatively well behaved. It should be noted, that not only does angular velocity noise cause delayed convergence and oscillation in the rotation estimate, it also induces an offset error in the position estimate.

Analysis of the effects of noise on other sensor yields less dramatic results. Noise on the orientation sensor delayed convergence of the rotation component and causes oscillations around the set point. Similarly, noise on the position or linear velocity sensors causes oscillations around the set point, though it did not delay convergence.

Changing the estimate dynamics to those of proposition 3 resulted in the temporary divergence of the position while the angular slope is high, as depicted in figure 5.

Under high angular noise, the modified form of $\hat{V}$ remains stable, undergoing little additional disturbance than the standard form, as depicted in figure 6.

VIII. EXPERIMENTAL RESULTS

We applied the filter developed in section V to experimentally obtained data to analyse the real world performance of the algorithm. We used experimental data obtained by Thibault Cheviron [3] from a radio controlled helicopter in hover over a visual target. The experimental platform consists of a Microstrain 3DMG IMU and a Philips Webcam mounted on a Vario Benzin-Acrobatic 23cc radio controlled helicopter, as depicted in figure 7. The inertial sensor data is acquired

at a rate of 50 Hz, and vision measurements at a rate of 10 Hz.

Data from the Vision and IMU measurements were harmonised, to place them in the same (body fixed) frame of reference, and the filter applied. The pose estimate was initiated at no rotational or position offset. Filter gains of $K_R = 1$ and $K_P = 10$ were selected by hand tuning. A prefilter was used to estimate velocity from acceleration and pose measurements. No bias correction was performed on either the gyrometer measurements or velocity estimate.

The results obtained using the experimental data are depicted in figures 8 and 9. These graphs compare estimate from the 3DMG IMU's industrial filter, vision measurements and our filter. As can be seen, our filter quickly overcomes the error in initial conditions and tracks the moving target well.

IX. CONCLUSIONS

In this paper we have provided theoretical developments for both a direct and complementary filter, evolving directly on the SE(3) manifold with exponential convergence. We developed methods for practical implementation of these filters and identify theoretically based guidelines for gain selection.

We provided simulations analysing the effects of noise in various sensor measurements on the complementary filter.
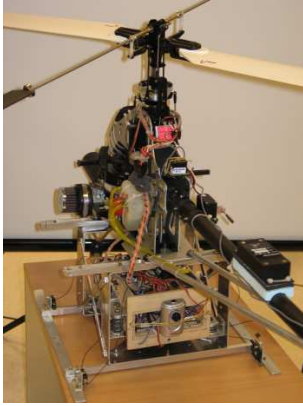
We identified a high set-point sensitivity to angular velocity noise, and a moderate convergence time sensitivity to orientation sensor noise.

We provided experimental results verifying the operation of our filter on real world data.

Fig. 7. Experimental Platform: Vario Benzin-Acrobatic 23cc radio controlled helicopter, fitted with low-cost, lightweight camera and IMU.
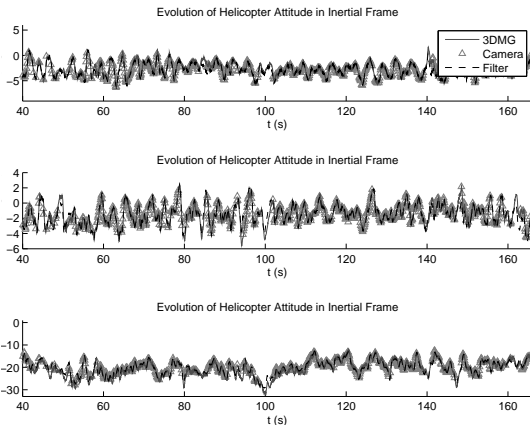

Fig. 8. Attitude estimate from experimental results, comparing estimates from the IMU's industrial filter, vision measurements and our filter.
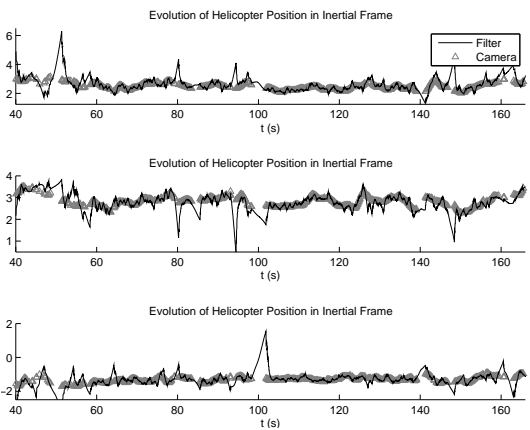

Fig. 9. Position estimate from experimental results, comparing estimates from vision measurements and our filter.

REFERENCES

[1] O. Amidi, T. Kanade, and R. Miller. *Vision-based autonomous helicopter research at Carnegie Mellon robotics institute (1991-1998)*, chapter 15, pages 221–232. IEEE press and SPIE Optical Engineering press, New York, USA, 1999. Edited by M. Vincze and G. D. Hager.

[2] Mitch Bryson and Salah Sukkarieh. Vehicle model aided inertial navigation for a UAV using low-cost sensors. In *Proceedings of the Australasian Conference on Robotics and Automation*, http://www.araa.asn.au/acra/acra2004/index.html (visited 7 March 2005), 2004. Australian Robotics and Automation Association.

[3] T. Cheviron, T. Hamel, R. Mahony, and G. Baldwin. Robust nonlinear fusion of inertial and visual data for position, velocity and attitude estimation of uav. 2006. Submitted to ICRA07.

[4] Peter Corke, Jorge Dias, Markus Vincze, and Jorge Lobo. Integration of vision and inertial sensors. In *Proceedings of the IEEE International Conference on Robotics and Automation, ICRA '05.*, number W-M04, Barcellona, Spain, April 2005. Full day Workshop.

[5] E. Frazzoli, M.A. Dahleh, and E. Feron. *Advances in Systems Theory*, chapter A Hybrid Control Architecture for Aggressive Maneuvering of Autonomous Aerial Vehicles. Kluwer Academic Publishers, 1999.

[6] Tarek Hamel and Robert Mahony. Attitude estimation on SO(3) based on direct inertial measurements. Institue of Electrical and Electronic Engineers, 2006.

[7] Jorge Lobo and Jorge Dias. Vision and inertial sensor cooperation using gravity as a vertical reference. *IEEE Transactions on Pattern Analysis and Machine Intelligence*, 25(12):1597–1608, 2003.

[8] Robert Mahony, Tarek Hamel, and Jean-Michel Pflimlin. Complementary filter design on the special orthogonal group SO(3). Institute of Electrical and Electronic Engineers, December 2005.

[9] Joo Lus Marins, Xiaoping Yun, Eric R. Bachmann, Robert B. McGhee, and Michael J. Zyda. An extended kalman filter for quaternion-based orientation estimation using marg sensors. 2001.

[10] Richard M. Murray, Zexiang Li, and S. Shankar Sastry. *A Mathematical Introduction to Robotic Manipulation*. CRC Press, 2000 Corporate Blvd., N.W., Boca Raton, Florida 33431, 1993.

[11] Henrik Rehbinder and Bikoy K. Ghosh. Pose estimation using line-based dynamic vision and inertial sensors. *IEEE Transaction on Automatic Control*, 48(2):186–199, 2003.

[12] Henrik Rehbinder and Xiaoming Hu. Drift-free attitude estimation for accelerated rigid bodies. In *Proceedings 2001 ICRA. IEEE International Conference on Robotics and Automation*, 2001.

[13] J. Roberts, P. Corke, and G. Buskey. Low-cost flight control system for a small autonomous helicopter. In *Proceedings of the Australasian Conference on Robotics and Automation, ACRA02*, Auckland, New-Zealand, 2002.

[14] S. Salcudean. A globally convergent angular velocity observer for rigid body motion. *IEEE Transactions on Automatic Control*, 46, no 12:1493–1497, 1991.

[15] S. Saripalli, J.M. Roberts, P.I. Corke, and G. Buskey. A tale of two helicopters. In *Proceedings of the IEEE/RSJ Interntational Conference on Intelligent Robots and Systems*, pages 805–810, Las Vegas, Oct. 2003.

[16] J. Thienel and R. M. Sanner. A coupled nonlinear spacecraft attitude controller and observer with an unknown constant gyro bias and gyro noise. *IEEE Transactions on Automatic Control*, 48(11):2011 – 2015, Nov. 2003.

[17] B. Vik and T. Fossen. A nonlinear observer for GPS and INS integration. In *Proceedings of the 40th IEEE Conference on Decision and Control*, 2001.

[18] Markus Vincze, Jorge Dias, Peter Corke, Stefan Chroust, and Jorge Lobo. Integration of vision and inertial sensors. In *Proceedings of the 11th International Conference on Advanced Robotics, ICAR '03*, Coimbra, Portugal, July 2003. half day Workshop.

[19] Eric W. Weisstein. Runge-Kutta method. From MathWorld– A Wolfram Web Resource. http://mathworld.wolfram.com/Runge-KuttaMethod.html. Accessed 28 September 2006.